Diffraction control in periodically curved two-dimensional waveguide arrays

Ivan L. Garanovich[1], **Alexander Szameit**[2], **Andrey A. Sukhorukov**[1],
Thomas Pertsch[2], **Wieslaw Krolikowski**[1], **Stefan Nolte**[2],
Dragomir Neshev[1], **Andreas Tuennermann**[2], **and Yuri S. Kivshar**[1]

[1]*Centre for Ultra-high bandwidth Devices for Optical Systems (CUDOS),
Nonlinear Physics Centre and Laser Physics Centre,
Research School of Physical Sciences and Engineering, Australian National University,
Canberra, ACT 0200, Australia*
[2]*Institute of Applied Physics, Friedrich-Schiller-University Jena,
Max-Wien-Platz 1, 07743 Jena, Germany*

ilg124@rsphysse.anu.edu.au

http://www.rsphysse.anu.edu.au/nonlinear

Abstract: We study propagation of light beams in two-dimensional photonic lattices created by periodically curved waveguide arrays. We demonstrate that by designing the waveguide bending, one can control not only the *strength* and *sign* of the beam diffraction, but also to engineer the effective *geometry* and even *dimensionality* of the two-dimensional photonic lattice. We reveal that diffraction of different spectral components of polychromatic light can display completely different patterns in the same periodically modulated structure, e.g. one-dimensional, hexagonal, or rectangular. Our results suggest novel opportunities for efficient self-collimation, focusing, and reshaping of light beams in two-dimensional photonic structures.

References and links

1. D. N. Christodoulides, F. Lederer, and Y. Silberberg, "Discretizing light behaviour in linear and nonlinear waveguide lattices," Nature **424,** 817–823 (2003).
2. A. L. Jones, "Coupling of optical fibers and scattering in fibers," J. Opt. Soc. Am. **55,** 261 (1965).
3. S. Somekh, E. Garmire, A. Yariv, H. L. Garvin, and R. G. Hunsperger, "Channel optical waveguide directional couplers," Appl. Phys. Lett. **22,** 46–47 (1973).
4. T. Pertsch, P. Dannberg, W. Elflein, A. Brauer, and F. Lederer, "Optical Bloch oscillations in temperature tuned waveguide arrays," Phys. Rev. Lett. **83,** 4752–4755 (1999).
5. R. Morandotti, U. Peschel, J. S. Aitchison, H. S. Eisenberg, and K. Silberberg, "Experimental observation of linear and nonlinear optical Bloch oscillations," Phys. Rev. Lett. **83,** 4756–4759 (1999).
6. N. Chiodo, G. Della Valle, R. Osellame, S. Longhi, G. Cerullo, R. Ramponi, P. Laporta, and U. Morgner, "Imaging of Bloch oscillations in erbium-doped curved waveguide arrays," Opt. Lett. **31,** 1651–1653 (2006).
7. H. Trompeter, T. Pertsch, F. Lederer, D. Michaelis, U. Streppel, A. Brauer, and U. Peschel, "Visual observation of Zener tunneling," Phys. Rev. Lett. **96,** 023901–4 (2006).
8. H. Trompeter, W. Krolikowski, D. N. Neshev, A. S. Desyatnikov, A. A. Sukhorukov, Yu. S. Kivshar, T. Pertsch, U. Peschel, and F. Lederer, "Bloch oscillations and Zener tunneling in two-dimensional photonic lattices," Phys. Rev. Lett. **96,** 053903–4 (2006).
9. A. Fratalocchi, G. Assanto, K. A. Brzdakiewicz, and M. A. Karpierz, "Optically induced Zener tunneling in one-dimensional lattices," Opt. Lett. **31,** 790–792 (2006).

10. S. Longhi, M. Marangoni, M. Lobino, R. Ramponi, P. Laporta, E. Cianci, and V. Foglietti, "Observation of dynamic localization in periodically curved waveguide arrays," Phys. Rev. Lett. **96,** 243901–4 (2006).

11. R. Iyer, J. S. Aitchison, J. Wan, M. M. Dignam, and C. M. de Sterke, "Exact dynamic localization in curved AlGaAs optical waveguide arrays," Opt. Express **15,** 3212–3223 (2007), http://www.opticsinfobase.org/abstract.cfm?URI=oe-15-6-3212.

12. G. Lenz, I. Talanina, and C. M. de Sterke, "Bloch oscillations in an array of curved optical waveguides," Phys. Rev. Lett. **83,** 963–966 (1999).

13. H. S. Eisenberg, Y. Silberberg, R. Morandotti, and J. S. Aitchison, "Diffraction management," Phys. Rev. Lett. **85,** 1863–1866 (2000).

14. G. Lenz, R. Parker, M. C. Wanke, and C. M. de Sterke, "Dynamical localization and AC Bloch oscillations in periodic optical waveguide arrays," Opt. Commun. **218,** 87–92 (2003).

15. S. Longhi, "Self-imaging and modulational instability in an array of periodically curved waveguides," Opt. Lett. **30,** 2137–2139 (2005).

16. I. L. Garanovich, A. A. Sukhorukov, and Yu. S. Kivshar, "Broadband diffraction management and self-collimation of white light in photonic lattices," Phys. Rev. E **74,** 066609–4 (2006).

17. J. Wan, M. Laforest, C. M. de Sterke, and M. M. Dignam, "Optical filters based on dynamic localization in curved coupled optical waveguides," Opt. Commun. **247,** 353–365 (2005).

18. J. D. Joannopoulos, R. D. Meade, and J. N. Winn, *Photonic Crystals: Molding the Flow of Light* (Princeton University Press, Princeton, 1995).

19. H. Kosaka, T. Kawashima, A. Tomita, M. Notomi, T. Tamamura, T. Sato, and S. Kawakami, "Self-collimating phenomena in photonic crystals," Appl. Phys. Lett. **74,** 1212–1214 (1999).

20. D. N. Chigrin, S. Enoch, C. M. S. Torres, and G. Tayeb, "Self-guiding in two-dimensional photonic crystals," Opt. Express **11,** 1203–1211 (2003), http://www.opticsinfobase.org/abstract.cfm?URI=oe-11-10-1203.

21. P. T. Rakich, M. S. Dahlem, S. Tandon, M. Ibanescu, M. Soljacic, G. S. Petrich, J. D. Joannopoulos, L. A. Kolodziejski, and E. P. Ippen, "Achieving centimetre-scale supercollimation in a large-area two-dimensional photonic crystal," Nat. Mater. **5,** 93–96 (2006).

22. U. Ropke, H. Bartelt, S. Unger, K. Schuster, and J. Kobelke, "Two-dimensional high-precision fiber waveguide arrays for coherent light propagation," Opt. Express **15,** 6894–6899 (2007), http://www.opticsinfobase.org/abstract.cfm?URI=oe-15-11-6894.

23. Y. G. Han and S. B. Lee, "Tunable dispersion compensator based on uniform fiber Bragg grating and its application to tunable pulse repetition-rate multiplication," Opt. Express **13,** 9224–9229 (2005), http://www.opticsinfobase.org/abstract.cfm?URI=oe-13-23-9224.

24. S. Nolte, M. Will, J. Burghoff, and A. Tuennermann, "Femtosecond waveguide writing: a new avenue to three-dimensional integrated optics," Appl. Phys. A **77,** 109–111 (2003).

25. T. Pertsch, U. Peschel, F. Lederer, J. Burghoff, M. Will, S. Nolte, and A. Tunnermann, "Discrete diffraction in two-dimensional arrays of coupled waveguides in silica," Opt. Lett. **29,** 468–470 (2004).

26. A. Szameit, D. Blomer, J. Burghoff, T. Schreiber, T. Pertsch, S. Nolte, A. Tunnermann, and F. Lederer, "Discrete nonlinear localization in femtosecond laser written waveguides in fused silica," Opt. Express **13,** 10552–10557 (2005), http://www.opticsinfobase.org/abstract.cfm?URI=oe-13-26-10552.

27. A. Szameit, D. Blomer, J. Burghoff, T. Pertsch, S. Nolte, and A. Tunnermann, "Hexagonal waveguide arrays written with fs-laser pulses," Appl. Phys. B **82,** 507–512 (2006).

28. P. G. Kevrekidis, B. A. Malomed, and Y. B. Gaididei, "Solitons in triangular and honeycomb dynamical lattices with the cubic nonlinearity," Phys. Rev. E **66,** 016609–10 (2002).

29. A. Szameit, T. Pertsch, F. Dreisow, S. Nolte, A. Tunnermann, U. Peschel, and F. Lederer, "Light evolution in arbitrary two-dimensional waveguide arrays," Phys. Rev. A **75,** 053814–14 (2007).

30. Y. V. Kartashov, L. Torner, and D. N. Christodoulides, "Soliton dragging by dynamic optical lattices," Opt. Lett. **30,** 1378–1380 (2005).

31. I. L. Garanovich, A. A. Sukhorukov, and Yu. S. Kivshar, "Soliton control in modulated optically-induced photonic lattices," Opt. Express **13,** 5704–5710 (2005), http://www.opticsinfobase.org/abstract.cfm?URI=oe-13-15-5704.

32. C. R. Rosberg, I. L. Garanovich, A. A. Sukhorukov, D. N. Neshev, W. Krolikowski, and Yu. S. Kivshar, "Demonstration of all-optical beam steering in modulated photonic lattices," Opt. Lett. **31,** 1498–1500 (2006).

33. C. Zener, Proc. R. Soc. London A **145,** 523–529 (1934).

1. Introduction

The physics of light propagation in photonic lattices such as arrays of weakly coupled parallel optical waveguides is attracting increasing interest in recent years [1]. In these structures, the classical light tunneling between the neighboring waveguides [2,3] closely resembles the quantum electron dynamics in crystalline potentials. Whereas the monitoring of the electron motion in crystals is a complicated problem, the optical beam reshaping can be observed directly in

real space. This has stimulated the experimental studies of optical analogs for a variety of phenomena originally predicted for quantum systems including Bloch oscillations [4–6], Zenner tunnelling [7–9] and dynamic localization [10, 11]. These effects are associated with the presence of external driving field which can be represented by a special modification of the photonic lattice by one of the following methods: (i) the transverse modulation of the photonic lattice, such as the waveguide strength and spacing [5] or the background refractive index [4, 8], or (ii) the bending of waveguides in the longitudinal direction [12]. An important advantage of the second approach is that the structure remains ideally periodic in the transverse direction, such that the beam propagation does not depend on the shift of the input location by several periods. On the other hand, the longitudinal bending profile can be selected independently to manage the strength and type of the beam diffraction [13–15].

The periodically curved waveguide arrays not only provide a means to study the fundamental wave phenomena, but can also find applications for spatial-spectral shaping of ultra-broadband optical signals, such as the supercontinuum radiation [16]. This possibility arises because the strength of effective driving force experienced by the beam is proportional to the optical wavelength, allowing one to observe different diffraction regimes in the same structure [10] with potential applications for signal filtering [17]. The characteristic longitudinal bending periods in such structures are of the order of millimeters, supporting adiabatic beam evolution along the structure in a broad spectral region. This is different from the photonic crystals [18] featuring two- and three-dimensional modulation of the optical refractive index on the order of the wavelength, where the diffraction can only be optimized in a specific spectral window around the resonant wavelength [19–21].

The effect of periodic bending has been only studied for one-dimensional arrays of optical waveguides. On the other hand, fabrication of two-dimensional high-precision fiber waveguide arrays for coherent light propagation has been recently reported [22]. Possibility to create various bended structures with optical fibers has been demonstrated experimentally, see e.g [23] and references therein. Also, recent advances in waveguide fabrication with femtosecond laser writing technique [24–27] make it possible to realize structures of arbitrary two-dimensional geometry.

In this work, we study, for the first time to our knowledge, the effect of periodic waveguide bending on beam propagation in two-dimensional waveguide arrays. We show that by an appropriate choice of bending geometry, one can control the beam shaping in novel ways. In particular, the beam diffraction and propagation along the different lattice directions can be controlled independently. Moreover, the light evolution can be made significantly different depending on the optical wavelength.

2. Beam evolution in periodically curved two-dimensional waveguide arrays

2.1. Generalized tight-binding approximation

We study propagation of optical beams in a two-dimensional array of coupled optical waveguides [see Fig. 1(a)], where the waveguide axes are periodically curved in the longitudinal propagation direction [see an example in Fig. 1(b)]. In the linear regime, the beam dynamics is defined by the independent evolution of the complex envelopes $E(x, y, z)$ of the electric field at the different optical wavelengths λ. In the case of weak refractive index contrast, which is satisfied for the laser-written structures in glass [26], the field evolution is governed by the normalized paraxial equation,

$$i\frac{\partial E}{\partial z} + \frac{\lambda}{4\pi n_0} \left(\frac{\partial^2 E}{\partial x^2} + \frac{\partial^2 E}{\partial y^2} \right) + \frac{2\pi}{\lambda} v\left[x - x_0(z), y - y_0(z)\right] E = 0. \tag{1}$$
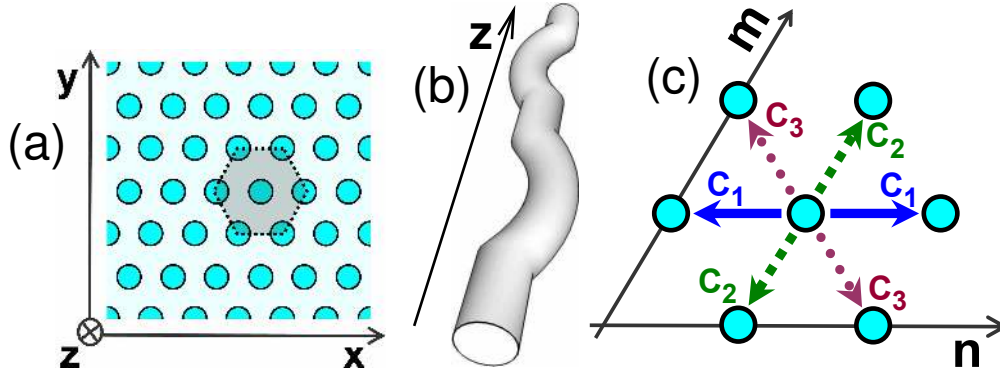
Fig. 1. (1.2MB) Sketch of modulated hexagonal photonic lattice. (a) Two-dimensional cross-section. Shading marks the unit cell, each lattice site has six nearest neighbors. (b) Schematic of the individual waveguide with the axis periodically curved in the z-direction. (c) Couplings between the nearest neighbours in the hexagonal lattice. Lattice sites are numbered along the n and m-axes.

Here x and y are the transverse coordinates, z is the propagation coordinate, λ is the vacuum wavelength, c is the speed of light, and n_0 is the average refractive index of the medium. The functions $x_0(z)$ and $y_0(z)$ determine the transverse shift of the whole lattice depending on the propagation distance z [see the lattice movement in the animations in Figs. 3-6]. The function $v(x,y)$ describes the refractive index modulation in the transverse cross-section. For the waveguide array, $v(x,y) = \sum_{n,m} v_0(x - x_{n,m}, y - y_{n,m})$, where $v_0(x,y)$ is the refractive index profile of a single waveguide, $(x_{n,m}, y_{n,m})$ are the waveguide positions at the input facet, and n and m are the discrete waveguide numbers [see Fig. 1(c)].

When the tilt of beams and waveguides at the input facet is less than the Bragg angle, the beam propagation is primarily characterized by coupling between the fundamental modes of the individual waveguides, and it can be described by the tight-binding coupled equations [10, 15]. Specifically, we represent the field as a sum of individual waveguide modes,

$$
\begin{aligned}
E = \sum_{n,m} &\Psi_{n,m}(z) E_0 [x - x_{n,m} - x_0(z), \, y - y_{n,m} - y_0(z), \, z] \\
&\exp\{2ip\dot{x}_0(z)[x - x_{n,m} - x_0(z)] + 2ip\dot{y}_0(z)[y - y_{n,m} - y_0(z)]\} \\
&\exp\left\{ip \int_0^z [\dot{x}_0(\xi)]^2 \, d\xi + ip \int_0^z [\dot{y}_0(\xi)]^2 \, d\xi\right\},
\end{aligned}
\tag{2}
$$

where $\Psi_{n,m}$ are the mode amplitudes, the dots stand for the derivatives, E_0 is the mode of individual straight waveguide, and $p = \pi n_0 / \lambda$. Following the standard procedure, we substitute Eq. (2) into Eq. (1), multiply the resulting expressions by $E_0^*[x - x_{n',m'} - x_0(z), \, y - y_{n',m'} - y_0(z), \, z]$, and integrate over the transverse dimensions (x,y). Then, in the leading order approximation we derive a set of coupled equations for the mode amplitudes,

$$
i\frac{d\Psi_{n,m}}{dz} + \sum_{n',m' \neq n,m} \widetilde{C}_{n,n',m,m'} \Psi_{n',m'} = 0,
\tag{3}
$$

where $\widetilde{C}_{n,n',m,m'} = \exp[-2ip\dot{x}_0(z)(x_{n',m'} - x_{n,m}) - 2ip\dot{y}_0(z)(y_{n',m'} - y_{n,m})] \int\int E_0[x - x_{n,m} - x_0(0), \, y - y_{n,m} - y_0(0), \, 0] E_0^*[x - x_{n',m'} - x_0(0), \, y - y_{n',m'} - y_0(0), \, 0][v(x, y) - v_0(x - x_{n,m}, y - y_{n,m})] \, dx \, dy / \int\int |E_0[x - x_{n,m} - x_0(0), \, y - y_{n,m} - y_0(0), \, 0]|^2 \, dx \, dy$. These expressions show that
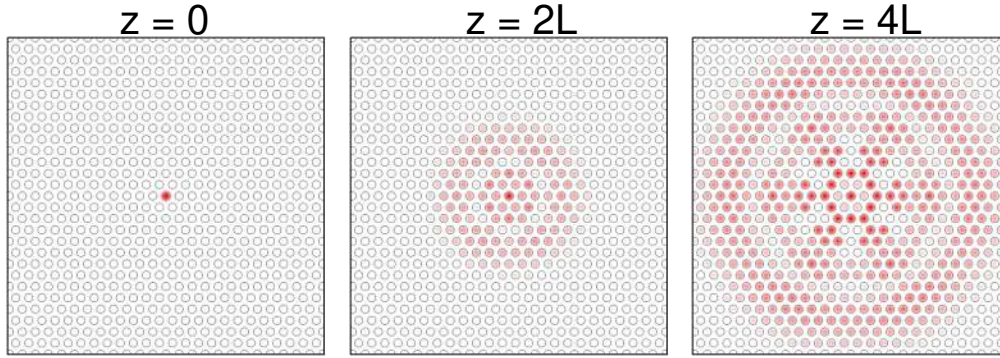
z = 0   z = 2L   z = 4L

Fig. 2. (1.2MB) Discrete diffraction in a hexagonal lattice of straight waveguides. Animation shows the patterns of the light-field distribution as the beam propagates over the distance $4L = 84$ mm. Wavelength is $\lambda = 633$ nm.

the effect of periodic bending appears through the modifications of phases of the coupling coefficients along the propagation direction z.

2.2. Discrete equations for hexagonal photonic lattices

In the case of a periodic hexagonal lattice, we take $x_{n,m} = d(n + m/2)$ and $y_{n,m} = dm\sqrt{3}/2$, where d defines the lattice period (see Fig. 1). When only the nearest-neighbor waveguide coupling is taken into account, Eqs. (3) are reduced to the following form,

$$i\frac{d\Psi_{n,m}}{dz} + \widetilde{C}_1^*\Psi_{n-1,m} + \widetilde{C}_1\Psi_{n+1,m} + \widetilde{C}_2^*\Psi_{n,m-1} + \widetilde{C}_2\Psi_{n,m+1} + \widetilde{C}_3^*\Psi_{n-1,m+1} + \widetilde{C}_3\Psi_{n+1,m-1} = 0,$$

(4)

where $\widetilde{C}_1 \equiv \widetilde{C}_{n,n+1,m,m} = C_1\exp[-i\omega\dot{x}_0(z)]$, $\widetilde{C}_2 \equiv \widetilde{C}_{n,n,m,m+1} = C_2\exp[-i\omega\dot{x}_0(z)/2 - i\omega\dot{y}_0(z)\sqrt{3}/2]$, $\widetilde{C}_3 \equiv \widetilde{C}_{n,n+1,m,m-1} = C_3\exp[-i\omega\dot{x}_0(z)/2 + i\omega\dot{y}_0(z)\sqrt{3}/2]$, and $\omega = 2\pi n_0 d/\lambda$ is the dimensionless frequency. The real-valued coefficients C_1, C_2, and C_3 define the coupling strength between the neighboring waveguides along the different high-symmetry directions in a hexagonal lattice [28] [see Fig. 1(c)], and they characterize diffraction in a straight hexagonal waveguide array with $x_0 \equiv 0$ and $y_0 \equiv 0$ [29] [see an example in Fig. 2]. When the lattice is composed of circular rods all coupling coefficients are the same, $C_1 = C_2 = C_3$. However, in the general case of non-symmetric waveguides, the transverse cross-section coupling coefficients along different directions may be all different [27].

3. Diffraction management in modulated hexagonal lattices

In order to specifically distinguish the effects due to diffraction management, we consider the light propagation in the waveguide arrays with symmetric bending profiles, since asymmetry may introduce other effects due to the modification of refraction, such as beam dragging and steering [30–32]. Specifically, we require that $x_0(z) = f_1(z - z_a)$ and $y_0(z) = f_2(z - z_a)$ for a given coordinate shift z_a, where functions $f_1(z)$ and $f_2(z)$ are symmetric, $f_1(z) \equiv f_1(-z)$, and $f_2(z) \equiv f_2(-z)$. Then, by analyzing the plane-wave solutions of Eqs. (4) using the approach developed for one-dimensional periodically curved waveguide arrays [10, 15, 16], it can be shown that after the full bending period [$z \to z + L$, where $x_0(z) \equiv x_0(z + L)$ and $y_0(z) \equiv y_0(z + L)$] the beam diffraction in the periodically curved hexagonal waveguide array is the same as in

a straight hexagonal waveguide array with the effective coupling coefficients

$$C_{1\mathrm{eff}} = C_1 L^{-1} \int_0^L \cos\left[\omega \dot{x}_0(\zeta)\right] d\zeta, \tag{5}$$

$$C_{2\mathrm{eff}} = C_2 L^{-1} \int_0^L \cos\left[\frac{\omega}{2}\dot{x}_0(\zeta) + \frac{\sqrt{3}}{2}\omega \dot{y}_0(\zeta)\right] d\zeta, \tag{6}$$

$$C_{3\mathrm{eff}} = C_3 L^{-1} \int_0^L \cos\left[\frac{\omega}{2}\dot{x}_0(\zeta) - \frac{\sqrt{3}}{2}\omega \dot{y}_0(\zeta)\right] d\zeta. \tag{7}$$

Remarkably, the couplings along different high symmetry directions in a two-dimensional periodically curved lattice [see Fig. 1(c)] can be controlled *independently* of each other by designing appropriate bending profiles. Thus, it becomes possible to engineer not only the strength and the sign of the diffraction in periodically curved two dimensional lattices, but to control also the effective lattice *geometry* and even the *dimensionality* of the lattice, as we demonstrate below.

We explore possibilities for the diffraction management in curved hexagonal lattices with a periodic waveguide bending profile which consists of alternating sinusoidal segments,

$$x_0(z) = \begin{cases} A_1\{\cos\left[2\pi z/z_0\right] - 1\}, & \text{if } 0 \leq z \leq z_0 \\ A_2\{\cos\left[2\pi(z - z_0)/(L/2 - z_0)\right] - 1\}, & \text{if } z_0 \leq z \leq L/2 \end{cases} \tag{8}$$

$$y_0(z) = \begin{cases} B_1\{\cos\left[2\pi z/z_0\right] - 1\}, & \text{if } 0 \leq z \leq z_0 \\ B_2\{\cos\left[2\pi(z - z_0)/(L/2 - z_0)\right] - 1\}, & \text{if } z_0 \leq z \leq L/2, \end{cases} \tag{9}$$

and $x_0(z) = -x_0(z - L/2)$, $y_0(z) = -y_0(z - L/2)$, for $L/2 \leq z \leq L$. At each point z the lattice is shifted as a whole in the transverse (x,y) plane along certain directions which are determined by the relative values of the amplitudes A_1 and B_1, or A_2 and B_2. The effective couplings in such structure can be calculated analytically in terms of Bessel functions

$$C_{1\mathrm{eff}} = 2C_1 L^{-1}\left[z_0 J_0\left(\tilde{\xi}_1\right) + \left(\frac{L}{2} - z_0\right) J_0\left(\tilde{\xi}_2\right)\right], \tag{10}$$

$$C_{2\mathrm{eff}} = 2C_2 L^{-1}\left[z_0 J_0\left(\frac{\tilde{\xi}_1}{2} + \frac{\sqrt{3}}{2}\bar{\xi}_1\right) + \left(\frac{L}{2} - z_0\right) J_0\left(\frac{\tilde{\xi}_2}{2} + \frac{\sqrt{3}}{2}\bar{\xi}_2\right)\right], \tag{11}$$

$$C_{3\mathrm{eff}} = 2C_3 L^{-1}\left[z_0 J_0\left(\frac{\tilde{\xi}_1}{2} - \frac{\sqrt{3}}{2}\bar{\xi}_1\right) + \left(\frac{L}{2} - z_0\right) J_0\left(\frac{\tilde{\xi}_2}{2} - \frac{\sqrt{3}}{2}\bar{\xi}_2\right)\right], \tag{12}$$

where $\tilde{\xi}_1 = 2\pi\omega A_1/z_0$, $\tilde{\xi}_2 = 2\pi\omega A_2/(L/2 - z_0)$, and $\bar{\xi}_1 = 2\pi\omega B_1/z_0$, $\bar{\xi}_2 = 2\pi\omega B_2/(L/2 - z_0)$.

Below we consider the case of the *planar waveguide bending*, when either $z_0 = L/2$, or $A_1 = B_1 = 0$. Then the direction in which the lattice shift occurs is the same along the whole length of the array, which is easier to realize experimentally. We flip the signs of the shifts $x_0(z)$ and $y_0(z)$ within each bending period to make the bending profiles symmetric in order to avoid asymmetric beam distortion due to higher-order effects such as third-order diffraction. Additionally, the waveguides are not tilted at the input, $\dot{x}_0(z=0) \equiv 0$ and $\dot{y}_0(z=0) \equiv 0$, in order to suppress excitation of higher-order photonic bands by incident beams inclined by less than the Bragg angle. The effect of Zener tunneling to higher bands [7, 8, 33] and associated scattering losses can be suppressed irrespective of the waveguide tilt inside the photonic structure by selecting sufficiently slow waveguide modulation in order to minimize the curvatures $\ddot{x}_0(z)$ and $\ddot{y}_0(z)$, and thereby achieve adiabatic beam shaping.

In the numerical simulations presented below, we consider the lattice where the individual waveguides are cylindrical rods with the Gaussian refractive index distribution with radius r
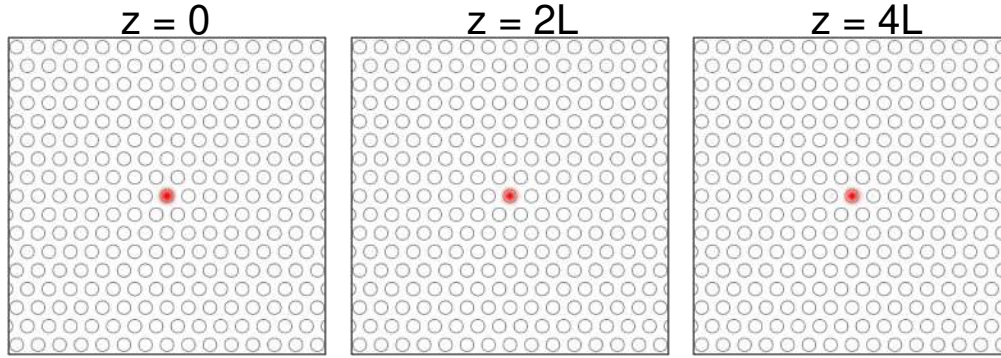
Fig. 3. (2.4MB) Self-collimation in a modulated hexagonal lattice. The field distribution is shown at the input, and after the propagation for two and four bending periods. Animation shows the beam propagation in a fixed viewpoint. Wavelength is $\lambda = 633$ nm.

within the rod cross-section. The refractive index contrast at the rod centers is δn, and the lattice spacing is d. For Figs. 3-5, we use the following lattice parameters which are typical for the experiments with waveguide arrays written in glass [26]: $d = 16$ μm, $r = 5$ μm, and $\delta n = 1.6 \cdot 10^{-3}$. The lattice parameters in Fig. 6 are $d = 8$ μm, $r = 2.5$ μm, and $\delta n = 6.4 \cdot 10^{-3}$. We take the refractive index of glass to be $n_0 = 1.46$. Waveguides are excited at the input with a Gaussian beam with the half width equal to the rod radius.

4. Self-collimation in modulated photonic lattices

First, we demonstrate the possibility for *two dimensional self-collimation* of light beams in periodically curved hexagonal photonic lattices. Self-collimation regime is realized when the diffraction is suppressed and all the effective coupling coefficients vanish, $C_{1\text{eff}} = C_{2\text{eff}} = C_{3\text{eff}} = 0$. We find that self-collimation becomes possible in a hexagonal lattice with a periodic bending profile which consists of alternating straight and sinusoidal segments [see an example in Fig. 1 (b)] such that $y_0(z) \equiv 0$, $z_0 = [1 - 1/J_0(\tilde{\xi})]^{-1}L/2$, $A_1 = 0$, $A_2 = -z_0\tilde{\xi}/\pi\omega J_0(\tilde{\xi})$, where J_0 is the Bessel function of the first kind of zero order, and $\tilde{\xi} \simeq 2.61$ is determined from the equation $J_0(\tilde{\xi}) = J_0(2\tilde{\xi})$. Then the lattice shift occurs along x-axis, and for the bending period $L = 21$ mm the self-collimation is realized when $z_0 = 0.98$ mm and $A_2 = 34$ μm, see Fig. 3.

In Fig. 3 one can see that the beam profile is exactly restored after propagation through each bending period [compare this figure with Fig. 2, where light beam spreads over many lattice sites after propagation for the same distance in the exactly the same but straight hexagonal waveguide array]. This effect is similar to the one dimensional self-collimation which was previously observed in one dimensional waveguide arrays with zigzag [13] and sinusoidal [10] bending profiles.

5. One-dimensional diffraction in two-dimensional lattices

Because couplings along different directions [see Fig. 1(c)] in a periodically curved hexagonal photonic lattice can be controlled independently [Eqs. (5)-(7)], it becomes possible to completely cancel the diagonal couplings, $C_{2\text{eff}} = C_{3\text{eff}} = 0$, while not changing the coupling in the horizontal direction, $C_{1\text{eff}} = C_1$. This can be realized with a simple sinusoidal bending of waveguide axes in y-direction, $x_0(z) \equiv 0$, $z_0 = L/2$, and $B_1 = \xi_1 L/2\sqrt{3}\pi\omega$, where $\xi_1 \simeq 2.40$ is the first root of the Bessel function J_0 [see Eqs. (10)-(12)]. For example, $B_1 = 20$ μm for $L = 21$ mm. Then, the light beam experiences a *one dimensional* discrete diffraction [13] dur-
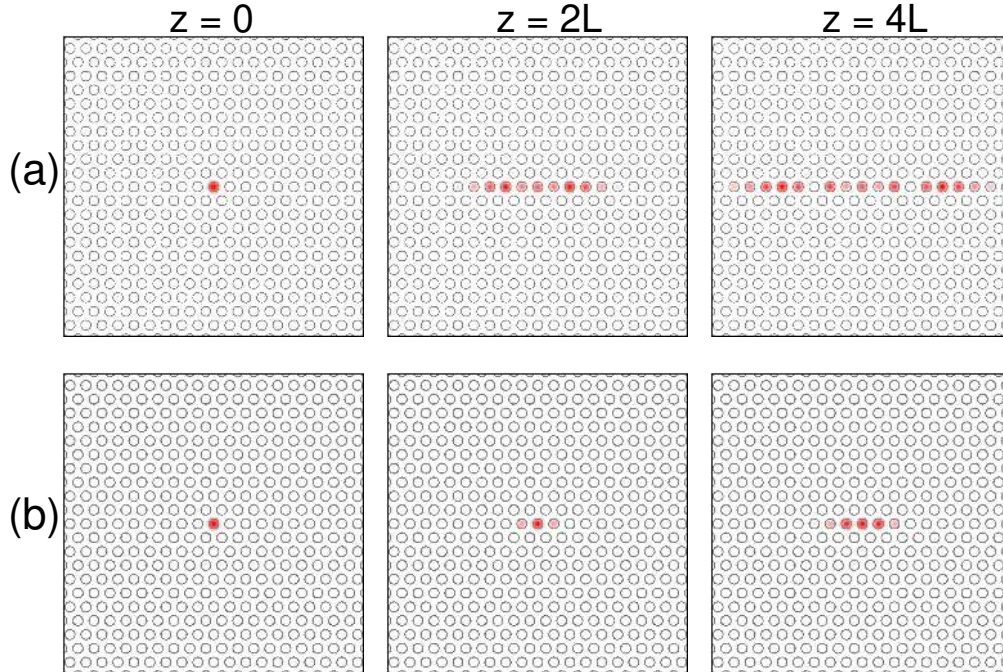
Fig. 4. One-dimensional diffraction in a modulated hexagonal lattice. The field distribution is shown at the input, and after the propagation for two and four bending periods. (a) (2.3MB) Lattice shift occurs in the y-direction. (b) (2.3MB) Lattice shift occurs in the x-direction. Animations show the propagation dynamics in a fixed viewport. Wavelength is $\lambda = 633$ nm.

ing propagation in such a periodically curved two-dimensional photonic lattice [see Fig. 4(a) where despite some coupling to the upper and lower lattice rows which is visible in the animation between the periods, the beam diffraction becomes exactly one dimensional after each period of propagation].

Interestingly, the same diagonal couplings $C_{2\mathrm{eff}}$ and $C_{3\mathrm{eff}}$, which determine essentially the coupling in the *vertical* direction to the upper and lower lattice rows [see Fig. 1(c)], can be canceled by the lattice shifts in only the *horizontal* x-direction as well. This is realized for the bending profile such that $y_0(z) \equiv 0$, $z_0 = L/2$, and $A_1 = \xi_1 L/2\pi\omega$. Then $A_1 = 35$ μm for $L = 21$ mm [see Fig. 4(b)]. In this case, the sign of the horizontal coupling is reversed, and it is also reduced about four times, $C_{1\mathrm{eff}} = C_1 J_0(2\xi_1) \simeq -0.24 C_1$. This results in a much less beam diffraction after propagation the same length compared to the preceding case when the lattice shift took place in the vertical direction [compare Fig. 4(b) with Fig. 4(a)].

6. Rectangular diffraction in hexagonal lattices

One can also cancel independently just one of the three couplings in a hexagonal lattice, and thus obtain a coupling geometry which corresponds essentially to a *rectangular* lattice. For example, the diagonal coupling $C_{3\mathrm{eff}}$ can be canceled with the periodic sinusoidal bending profile such that the lattice is shifted along the direction of this coupling, $z_0 = L/2$, $A_1 = A\cos[60°] = A/2$, $B_1 = -A\sin[60°] = -\sqrt{3}A/2$, and $A = \xi_1 L/4\pi\omega$. Then $C_{3\mathrm{eff}} = 0$, while the two other couplings are reduced symmetrically, $C_{1,2\mathrm{eff}} = C_{1,2} J_0(\xi_1/2) \simeq 0.67 C_1$ [see Eqs. (10)-(12)]. Then, $A = 17$ μm, $A_1 = 8.7$ μm, and $B_1 = -15$ μm for $L = 21$ mm, see Fig. 5.
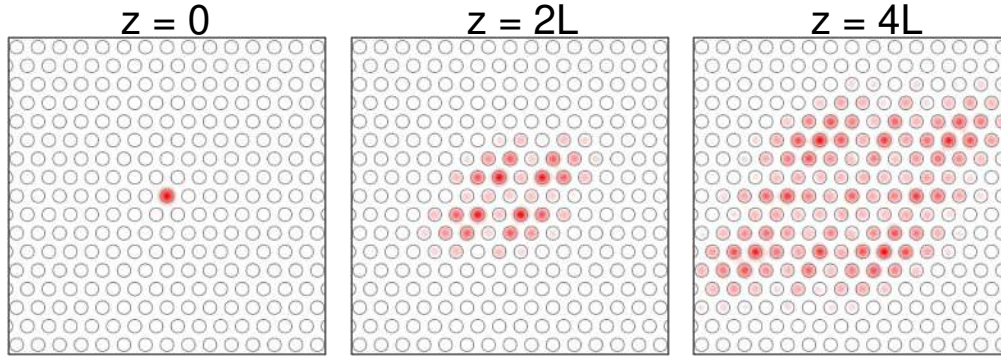
Fig. 5. (2.5MB) Rectangular diffraction in a modulated hexagonal lattice. The field distribution is shown at the input, and after the propagation for two and four bending periods. Animation shows beam propagation dynamics in a fixed viewport. Wavelength is $\lambda = 633$ nm.

In the movie in Fig. 5 one can see that despite the nontrivial beam evolution in between the periods, the diffraction pattern after each bending period is "rectangular", i.e. it is similar to diffraction patterns which are characteristic of the discrete diffraction in square and rectangular photonic lattices, where each lattice site is coupled to four nearest neighbors.

7. Propagation of polychromatic beams in modulated photonic lattices

Finally, we examine diffraction of multicolor light beams in modulated two-dimensional photonic lattices. In Eqs. (5)-(7) the value of the effective couplings depends not only on the specific bending profile $x_0(z)$ and $y_0(z)$, but also on the frequency ω, similar to the bending-induced coupling dispersion which appears in one-dimensional periodically curved waveguide arrays [16]. This means that different frequency components may experience very different types of diffraction in *the same* physical structure. This feature provides unique opportunities for the control and reshaping of polychromatic light beams in two dimensional photonic lattices. To illustrate this effect, we consider the propagation of light beams of different wavelengths in the same modulated hexagonal lattice with a simple sinusoidal bending profile, $y_0(z) \equiv 0$, $z_0 = L/2$, which is similar to the bending profile that we used above for demonstrating one-dimensional diffraction in a hexagonal lattice [see Fig. 4(b)].

Then from Eqs. (10)-(12) it follows that for the light wavelength such that the normalized frequency is $\omega_1 = \xi_1 L/2\pi A_1$, the diagonal couplings vanish, $C_{2\mathrm{eff}} = C_{3\mathrm{eff}} = 0$, while the horizontal coupling is reduced, $C_{1\mathrm{eff}} = C_1 J_0(2\xi_1) \simeq -0.24C_1$, and the beam at this wavelength will experience a *one dimensional* diffraction, as shown in Fig. 6(a). In this example, some coupling to upper and lower lattice rows also takes place. This is due to high-order coupling and increased scattering effects, which are the strongest for the longest wavelengths. We expect that the high-order coupling can be suppressed in modulated lattices by a special design of waveguide bending profiles, similar to results demonstrated for one-dimensional waveguide arrays [11].

On the other hand, for the frequency $\omega_2 = \tilde{\xi} L/2\pi A_1$, all three couplings are reduced simultaneously by the same factor $C_{1,2,3\mathrm{eff}} = C_{1,2,3} J_0(\tilde{\xi}) \simeq -0.10C_{1,2,3}$, and the symmetry of the original hexagonal lattice is exactly preserved, see Fig. 6(b) where the beam experiences reduced *hexagonal* diffraction.

For the frequency $\omega_3 = \xi_2 L/4\pi A_1$, where ξ_2 is the second root of the function J_0, the horizontal coupling is canceled $C_{1\mathrm{eff}} = 0$, while the diagonal couplings are reduced symmetrically
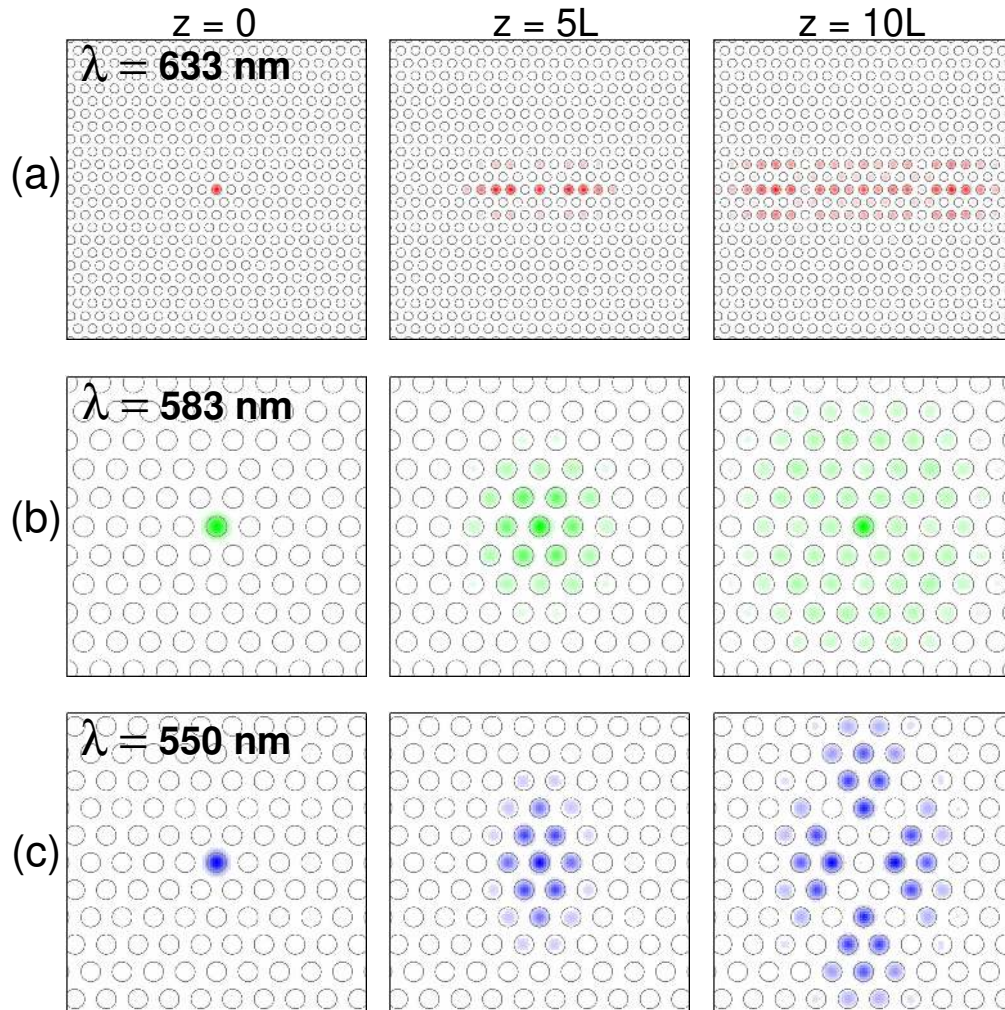
Fig. 6. Examples of different diffraction patterns in *the same* modulated hexagonal lattice. (a) (2.2MB) One-dimensional diffraction for the wavelength $\lambda = 633$ nm. (b) (2.3MB) Hexagonal diffraction for the wavelength $\lambda = 583$ nm. (c) (2.3MB) Rectangular diffraction for the wavelength $\lambda = 550$ nm. Animations show the beam propagation dynamics in a fixed viewport. The bending period and amplitude are $L = 10.5$ mm and $A_1 = 35$ μm, respectively.

$C_{2,3\text{eff}} = C_{2,3}\text{J}_0(\xi_2/2) \simeq -0.17C_{2,3}$. Accordingly, the beam at this frequency experiences a *rectangular* diffraction [see Fig. 6(c)], similar to the case shown in Fig. 5.

8.   Conclusions

We have studied theoretically the linear propagation and diffraction of light beams in two-dimensional photonic lattices created by periodically-modulated waveguides. We have suggested that a specific design of the waveguide bending would allow not only to control both strength and sign of light diffraction but also to engineer the effective geometry and even dimensionality of the photonic lattice. We have demonstrated that different spectral components of polychromatic light beams can experience completely different types of diffraction, e.g. one-dimensional, hexagonal, or rectangular, in the same structure. Our results provide a solid background for the further experimental studies of modulated photonic lattices, and they suggest novel opportunities for efficient reshaping of light beams in two-dimensional photonic structures.